UCRL-52223

NUMERICAL SIMULATION OF TORNADO-BORNE MISSILE IMPACT

David K. Tu and Robert C. Murray

February 8, 1977

Prepared for U.S. Energy Research & Development Administration under contract No. W-7405-Eng-48

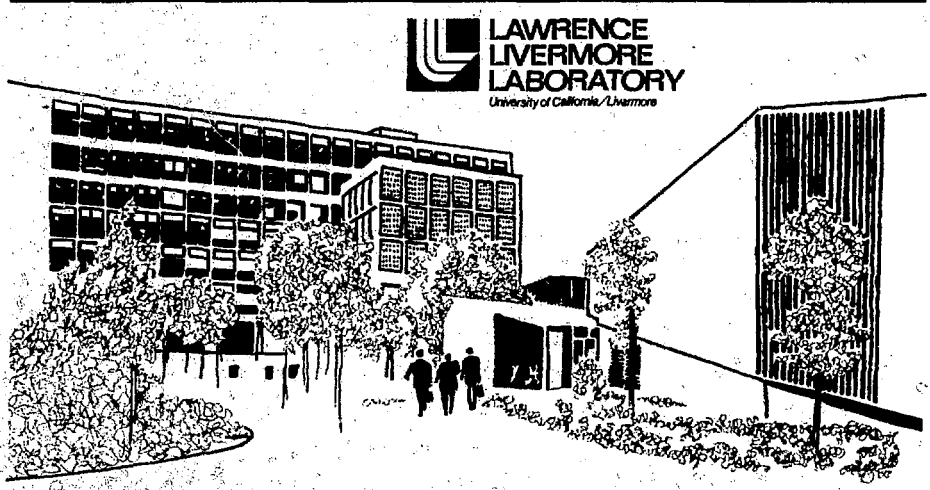

Printed in the United States of America
Available from
National Technical Information Service
U.S. Department of Commerce
5285 Port Royal Road
Springfield, VA 22161
Price: Printed Copy $; Microfiche $3.00

Page Range	Domestic Price	Page Range	Domestic Price
001–025	$ 3.50	326–350	10.00
026–050	4.00	351–375	10.50
051–075	4.50	376–400	10.75
076–100	5.00	401–425	11.00
101–125	5.50	426–450	11.75
126–150	6.00	451–475	12.00
151–175	6.75	476–500	12.50
176–200	7.50	501–525	12.75
201–225	7.75	526–550	13.00
226–250	8.00	551–575	13.50
251–275	9.00	576–600	13.75
276–300	9.25	601–up	*
301–325	9.75		

*Add $2.50 for each additional 100 page increment from 601 to 1,000 pages; add $4.50 for each additional 100 page increment over 1,000 pages.

Distribution Category
UC-11

LAWRENCE LIVERMORE LABORATORY
University of California Livermore, California 94550

UCRL-52223

NUMERICAL SIMULATION OF TORNADO-BORNE MISSILE IMPACT

David K. Tu

Robert C. Murray

MS. date: February 8, 1977

Contents

NUMERICAL SIMULATION OF TORNADO-BORNE MISSILE IMPACT

Abstract

In this study, we assessed the feasibility of using a finite element procedure to examine the impact phenomenon of a tornado-borne missile impinging on a reinforced concrete barrier.

The major emphasis of this study was to simulate the impact of a nondeformable missile. Several series of simulations were run, using an 8-in.-diam steel slug as the impacting missile. The numerical results were then compared with experimental field tests and empirical formulas.

Introduction

Presently, tornado design practices for fuel reprocessing and fuel fabrication facilities relate primarily to nuclear power plants.[1-3] Recently, the validity and conservatism of the accepted analytical methods used to assess the impact hazards of tornado-borne missiles have been questioned, particularly as they apply to fuel facilities.

When impact hazards of tornado-borne missiles are assessed, two general categories of investigation can be distinguished: local dynamic response and overall dynamic response. For the type of walls typical of fuel facilities and for the type of missiles concerning the Nuclear Regulatory Commission (NRC), local dynamic response is the primary concern.

In examining the analytical procedure for local response, the most widely accepted methods are generally empirical. Uncertainties over these empirical methods arise from the dissimilarities between the type of missiles used to develop these empirical methods and those associated with tornadoes.

Even if these uncertainties could be justified, the application of these analytical methods may be overly conservative when applied to fuel type facilities. With fuel facilities, the structural systems important to the safety of the facility may not require the same degree of integrity as do those of nuclear power plants.

In various past efforts,[4-6] the details of target and projectile impact have been analyzed by means of two-dimensional, finite difference techniques. While good agreement with experimental observations has been achieved by using the finite difference procedure, its execution is cumbersome and costly.

Development of a more practical procedure is needed to allow the NRC to identify more readily the strength and weakness of the present design and analytical methods for tornado missile impact.

The primary purpose of this report is to study the feasibility of using a finite element method to assess the impact phenomenon of tornado missiles impinging on reinforced concrete targets.

This report is divided into six sections. In the first two sections, a discussion of the impact phenomenon and a brief description of the available experimental results are given. The next section provides a perspective and the basis for this study, as well as a description of the selected finite element code used in this study. In the fourth section, the constitutive models used to describe the missile and target are discussed. Finally, the results of several numerical simulations are presented.

Summary

This study shows the potential of using the finite element method as a practical analytical tool to examine impact phenomenon of tornado-borne missiles.

Results of the study indicate that the finite element technique is a feasible method to predict scabbing threshold thickness. Based upon comparison with actual field tests, the finite element method gives reasonable corresponding results. For a nondeformable impacting missile, the finite element method is a relatively accurate means of assessing the back-face scab damages.

Three sets of numerical simulations were conducted, the first of which compared the simulated-impact interaction of the missile and target models with experimental-test results. The second assessed the progression of damage for two target thickness due to increasing missile velocities. The third set made preliminary examination of the impact interaction of a deformable missile and reinforced-concrete target wall.

Agreement between experimental observations and numerical simulations were established for nondeformable missile impact. Constitutive models were found to be available to model both the impinging missile and the reinforced concrete target. Reinforcements of the concrete wall were best represented by increasing the tensile yield value of the back layer of the concrete model.

Due to a lack of knowledge of the dynamic shear and compaction failures in concrete, the assessment of damage of the concrete target was limited to

tensile failures. A better understanding of the dynamic shear and compression behaviors of concrete is needed before the total impact phenomenon can be assessed by the finite element method.

Impact Phenomenon

Upon contact with a reinforced concrete barrier, a tornado-borne missile will either pass through (perforate), be embedded in, or be deflected by the structural element (Fig. 1). The resulting damage profile is dependent on (1) the velocity of the missile; (2) the angle of incidence; and (3) the physical properties of the missile (mass, shape and material strength) and the reinforced concrete barrier (strength, thickness, etc.).

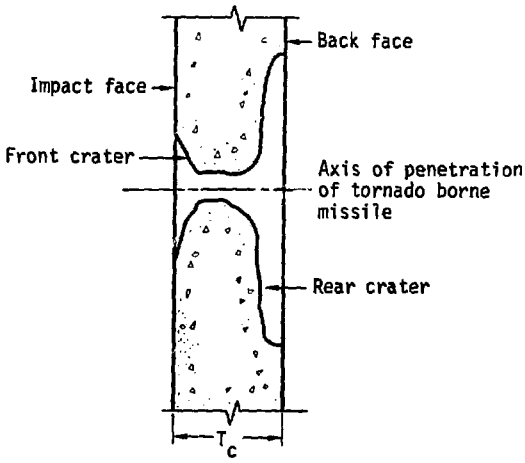

Fig. 1. Perforation of concrete due to tornado-borne missile.

When a missile contacts the surface of a reinforced concrete barrier, the pressures within the concrete reach the order of thousands of psi. If the missile can withstand this large interface pressure without deformation, the amount of penetration will be governed by the missile's mass, shape and strike velocity. If the missile does deform, the interface force will become effective over an increased cross-sectional area, thereby reducing the possible penetration for that missile.

If sufficient energy is transferred from the missile to the barrier, the back region surrounding the contact area will scab. This scabbing is the result of tension failure of the back-face concrete material.

The impact of the missile[7] on the front face of the barrier forms a compressive shock-wave front. This stress disturbance propagates through the concrete. When it reaches the backface of the barrier, a tension wave is reflected. If the tension stress in the reflected wave exceeds the tensile capacity of the concrete and the oncoming compression wave, the concrete will fracture, displacing material from the back-face of the barrier. The remaining stress waves will continue to fracture the concrete until the stress magnitude is reduced to the level below which no fracture will occur. A typical fracture profile of a reinforced concrete target at near scab threshold is shown in Fig. 2.

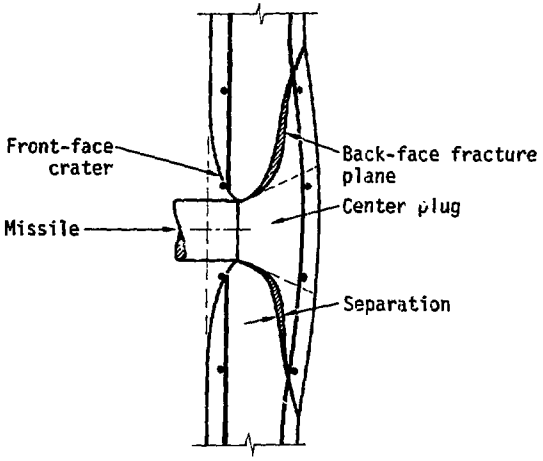

Fig. 2. Typical fracture planes[8] (impact velocity near threshold of scabbing).

The size and formation of the concrete scab fragment are attributed to the nonuniformity of the shock wave and the distortion of the wave as it propagates through the barrier. Additional damage is caused by shear cracks emanating from the front face. Radial cracks, induced by bending moments from inertia effects, weaken the back region further.[9]

Experimental Background

Equations currently used to evaluate the effects of tornado missile impact are generally empirical or semiempirical. Principally, all of the current equations[10] were developed for military applications, with experimental set-up oriented toward ordnance. Because of this, the experimental parameters supporting these empirical equations are limited in their similarities to tornado-type missiles. The reliability of using these empirical equations to assess tornado missile problems is uncertain.

The most commonly used equations in the United States are: (1) the Modified Petry formula, (2) the Army Corp of Engineers formula, (3) the Modified National Defense Research Committee formula, (4) the Amman and Whitney formula, and (5) the Ballistic Research Laboratory formula. All of the five equations were formulated from high-speed (500-2000 ft/sec) impact tests of nondeformable missiles designed for penetration. In comparison, missile consideration for nuclear facilities are generally in the lower-speed (0-500 ft/sec) region. Tornado missiles are also deformable to various degrees and are usually blunt-ended.

Recently, a number of experimental programs have examined the impact phenomenon of missiles associated with tornado hazards. The overall objectives of these programs were to examine the vulnerability of nuclear facilities to tornado missiles. The experimental programs have concentrated on the lower velocities and the large-diameter missiles which are of concern to the nuclear industry and nuclear regulatory agencies. Their results have allowed better assessment of existing empirical equations. They have also provided the framework for the development of existing and new analytical tools.

Two of the experimental programs are full-scale field tests. Calspan Corporation completed the first series of full-scale tests for Bechtel Corporation.[11] Sandia Laboratories completed a series of tests for ERDA[12] and the Electric Power Research Institute (EPRI).[13,14] These two tests have produced

important inroads into the determination of the vulnerability of nuclear facilities to tornado missiles. Brief descriptions of the two tests are found below.

Calspan Test Program[11]:

Calspan tests consisted of the following missiles:

- Wooden pole
- Steel slug
- Steel pipe.

All of Calspan's missiles were 8 in. in diameter. Except for two of the missiles, the approximate weight was 200 lb. The two exceptions were steel pipes weighing 132 lb. Velocities of these missiles were in the range of 100 to 500 ft/sec. Reinforced concrete test panels were 9 by 9 ft and had thicknesses of 12, 18 and 24 in. The concrete strength ranged from 4400 to 5800 psi.

Sandia Laboratories Test Program for EPRI[13,14]:

Sandia Laboratory tested four types of tornado-borne missiles.

- 1500-lb, 35-ft-long utility pole.
- 8-lb, 1-in., grade-60 reinforcing bar.
- 78-lb, 3-in., Schedule-40 pipe.
- 743-lb, 12-in., Schedule-40 pipe.

The reinforced concrete test panels were 12-, 18- and 24-in. thick. Panels were 17 by 17 ft in overall dimensions, with 15 by 15 ft free spans. The concrete strength was constructed to meet 3000 psi minimum design strength.

Comparison of experimental results with existing empirical equations has indicated that the Modified National Defense Research Committee (NDRC) formula is valid for predicting the depth of penetration and the scabbing thickness. In Kennedy's[10] comparison of predicted scabbing thicknesses and Calspan test results, Modified NDRC was consistently 20 to 35% higher than test results. The prediction of scabbing thickness by using other empirical equations was found to be inconsistent.

Further comparison of the Modified NDRC formula was done, using both Calspan and Sandia Laboratories test results. Use of the Modified NDRC formula gave good agreement with test results for the penetration of steel-pipe missiles. Also, the Modified NDRC formula gave good results for scabbing thickness predictions when the equivalent diameter of the pipe (based on actual pipe area) was used for the value of "d".

The Modified NDRC formula for missile penetration for steel slugs showed poor agreement with test results. However, for scabbing-thickness predictions the formula appears to be satisfactory.

None of the empirical equations were able to predict the response of wood-type missiles because of the highly deformable nature of these missiles. This highly deformable nature makes wood missiles no real threat to nuclear facilities — a conclusion confirmed by both Calspan and Sandia Laboratories large-scale tests.

Arising from the two full-scale experimental programs are two empirical equations that appear to be valid for tornado-type missiles: the Modified NDRC and Bechtel formulas.

Modified NDRC Formula[14]:

The Modified NDRC formula defines the depth of penetrations (x) by:

$$G_{(x/d)} = KN\, d^{0.20}\, W/d^3\, (V/1000)^{1.8},$$

where

$$G_{(x/d)} = \begin{cases} (x/2d)^2 & \text{for } x/d \leq 2.0 \\ (x/d-1) & \text{for } x/d \geq 2.0 \end{cases},$$

where

N = Missile shape factor (N = 0.72 for flat-nosed bodies),

d = Missile diameter (in.),

W = Missile weight (lb),

K = Concrete permeability factor = $180/\sqrt{f'_c}$,

f'_c = Ultimate compressive strength of concrete (psi),

V = Striking velocity of the missile (fps).

To determine scabbing thickness (t_s):

$$t_{s/d} = 7.91\ (x/d) - 5.06\ (x/d)^2 \text{ for } t/d < 3$$

$$t_{s/d} = 2.12 + 1.36\ (x/d) \text{ for } t/d > 3.$$

Bechtel Formula[8]:

Deriving the empirical relations directly from Calspan tests results, the Bechtel formula predicts scabbing thickness.

For steel-pipe missile,

$$T = 5.42\ \frac{W^{(0.4)} V^{(0.65)}}{\sqrt{f'_c}\, D^{(0.2)}}.$$

The solid steel missile

$$T = 15.5\ \frac{W^{(0.4)} V^{(0.5)}}{\sqrt{f'_c}\, D^{(0.2)}},$$

where

T = Thickness for threshold of spalling (in.),
W = Missile weight (lb),
D = Missile diameter (in.),
f'_c = Concrete strength (psi),
V = Missile velocity (fps).

The design thickness of a reinforced concrete element must be greater than that determined by the equations. An increase in thickness of 25% (which need not exceed 10 in.) is recommended.

Numerical Simulation

As stated earlier, the primary objective of this study is to determine the feasibility of using the finite element method to evaluate the impact interaction of tornado-borne missiles and reinforced concrete walls. Although certain empirical equations provide reasonable predictions of penetration and scabbing thickness, the equations describing impact do not use the constitutive properties of the target or the projectile. To make reasonable extensions of

the experimental data, a practical analytical tool incorporating the proper properties and considerations is needed.

Damage due to an impinging missile can be summarized as a combination of local- and overall-dynamic response. Since the impact time is short, relative to the fundamental period of the target structure, our predominant concern was with local response. Considering the various aspects of the local response, we feel the key to assuring the integrity of the structure from tornado-borne missiles is to prevent scabbing.

Since the onset of scabbing occurs within the first few hundred microseconds of impact, the most important aspect of the numerical procedure is to simulate the proper shock-interface conditions. We chose the HONDO program for this study because of its applicability to short-duration loadings.

CODE DESCRIPTION

HONDO[15] is a finite element code designed specifically to analyze extreme loadings incurred during accident conditions. Recent developments to HONDO by LLL have allowed the use of the program in examining the impact phenomenon of tornado-borne missiles.

HONDO is an explicit finite element code designed to calculate the large deformation, elastic and inelastic, dynamic transient response of plane or axisymmetric bodies of arbitrary shape and composition. To accommodate a variety of material composition, the program has eight constitutive relations. The explicit scheme allows the examination of the effects of short-duration loads at the early phases of the transient response. Artificial viscosity is employed to control the development of shocks incurred by impacts. In time, the program performs integration by use of a central-difference method, with the step size continuously monitored to maintain stability of the time integration scheme.

In general, finite element codes are not applicable to the solution of contact-impact problems because they lack the following capabilities required to adequately treat these problems:

- Shock-interface conditions to set correctly the velocity along the contact surface after a void closes.
- Sliding-material interfaces that allow sliding but not penetration.
- Tied-material interfaces that allow unequal zoning across the interface but no sliding.

- Friction .

To remedy this, a development effort was undertaken that has provided these capabilities in HONDO. Considerably more detail is provided by Hallquist.[16]

Description of Impacting Materials

MODELS

To isolate the impact phenomenon to the reinforced concrete target, we selected the simulation of nondeformable missile impact as the first step. The slug missile was chosen as the nondeformable impacting missile because of the available experimental results from Calspan Corporation[11] for comparisons.

Of the eight constitutive models available in HONDO, the elastic-plastic strain-hardening model was selected to model the nondeformable missile. We selected soil and crushable foam model to model the reinforced concrete target.

Nondeformable Missile

The elastic-plastic constitutive model was used to model the impacting missile.[15] The 8-in.-diam steel slug was characterized (Fig. 3) as a ductile material with a straight-line approximation for the elastic modulus (E) and yield stress (σ_y). The hardening parameter allows a linear combination of kinematic and isotropic hardening. When $\beta = 1$, isotropic hardening is obtained. The strain hardening modulus (E_t) is a straight-line approximation.

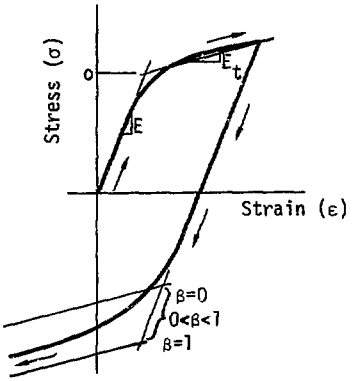

Fig. 3. Typical stress-strain behavior of a ductile metal bar.

Inside the yield surface, the material behaves elastically and isotropically. As the stress state contacts the yield surface, plastic straining occurs. A von Mises yield surface is used with a linear combination of isotropic and kinematic hardening behavior.

For the series of simulations using the non-deformable missile, the model missile was a 8-in.-diam steel slug, 14 in. in length, weighing 214 lb with a modulus of elasticity of 30×10^6 psi and a yield stress of 40×10^3 psi. The strain-hardening modulus was selected to be a third of the elastic modulus, with an isotropic hardening parameter.

Reinforced Concrete Target

The soil and crushable foam model was used to describe the reinforced concrete target. This model consists of an elastic-plastic isotropic constitutive relation for the pressure response of concrete.

The model allows for compaction and crushing of voids in the material and also a pressure-sensitive shear-failure behavior. These features are important characteristics of dynamic concrete behavior.

The yield surface used in this model is a surface of revolution in stress space, centered about the hydrostat with its open end pointing into compression. The open end is capped with a plane normal to the hydrostat. The deviatoric part (shear surface) is elastic-perfectly plastic and thus does not allow strain hardening. The volumetric part (compaction on cap surface) allows for variable strain hardening which is handled by allowing the plane normal to the hydrostat to move outward along the hydrostat. The yield surfaces in stress space are shown in Fig. 4.

Cap Surface

The volumetric hardening is described by

$$f_2 = p - f(\varepsilon_{kk}) .$$

For loading, $f_2 \geq 0$, $\dot{\varepsilon}_{kk} \leq 0$ increasing compression

$$p = f(\varepsilon_{kk}).$$

The function f, which describes the pressure-volume strain behavior, is shown in Fig. 5.

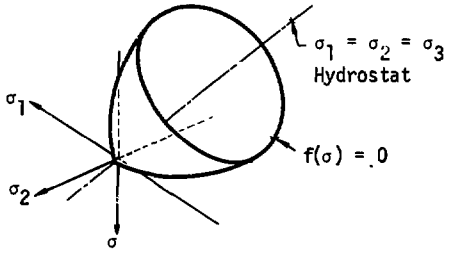

a) Shear yield surface in stress-space

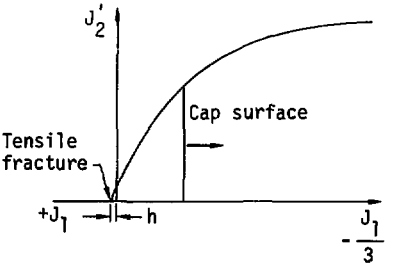

b) Cap surface in stress-space
J_1 = first invariant of the stress-sensor
J_2' = second invariant of the deviatoric stress-tensor

Fig. 4. Yield surface in stress-space.

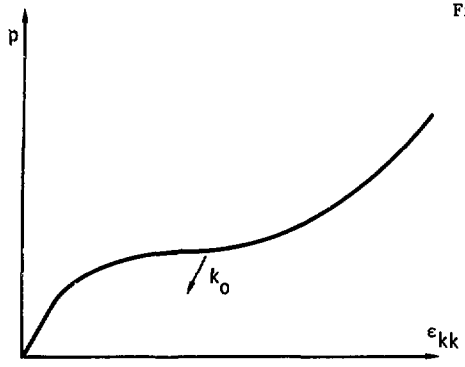

Fig. 5. Pressure-volumetric strain.

Tensile Fracture

Tensile fracture will occur if

$$p < h$$

where h is the minimum root of the polynomial $a_0 + a_1 p + a_2 p^2 = 0$ (refer to Fig. 4b).

Shear Surface

The shear surface is defined by a yield function of the form

$$f_1 = J_2' - \left(a_0 + a_1 p + a_2 p^2\right),$$

where

$$p = -1/3\ \sigma_{kk},$$

J_2' = Second Invariant of the Deviatoric-Stress Tensor.

In reviewing the literature,[17-20] two concrete models were found suitable to use in describing the shear yield surface of the soil and crushable foam model. One model was developed by Physics International (PI);[5] and the other model by Stanford Research Institute (SRI).[21]

PI, under contract with the Lawrence Livermore Laboratory (LLL), developed an inelastic model to assess the damage of a concrete wall impacted by a high-velocity projectile. PI's concrete model has a shear-yield surface in the form of

$$f_1 = \sqrt{3J_2'} - \left(a_0 + a_1 p + a_2 p^2\right).$$

where a_0, a_1 and a_2 are determined from experimental data. Data were assembled from the available literature and plotted as $\sqrt{3J_2'}$ versus p. A curve was fit through the data to determine the coefficients a_0, a_1 and a_2. (Fig. 6.) The resulting PI shear-yield function was determined to be

$$f_1 = \sqrt{3J_2'} - (2250 + 1.375\ p - 1.53 \times 10^{-5}\ p^2)$$

for p in pounds per square inch.

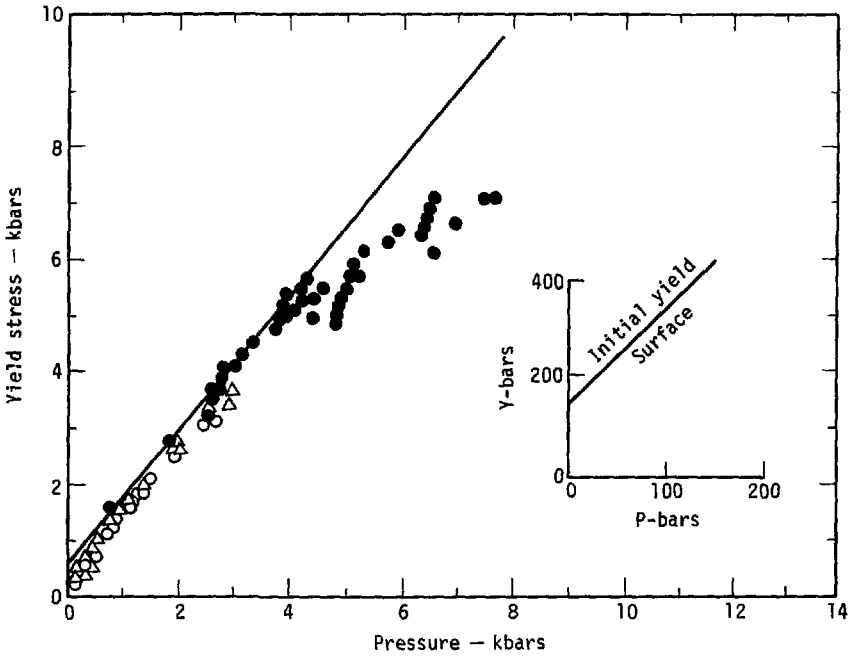

Fig. 6. Physics International shear-yield surface.

SRI, under contract with EPRI to investigate the tornado-borne missile problem, has developed a model describing the shear- and compaction-yielding characteristics of concrete. The parameters of the model were obtained from experiments conducted by SRI, and the model was tested by comparing its predicted response with the experimental data.

SRI's concrete model is built up from two yield surfaces. One describes the shear yielding and allows no hardening, while the other (cap surface) is used to describe the compaction yielding and allows isotropic work-hardening. The yield functions chosen are assumed to be functions of J_1 and J_2' and independent of J_3' (Fig. 7).

The form of the shear-yield surface is

$$f_1 = J_2' - (A - Be^{CJ_1}),$$

where

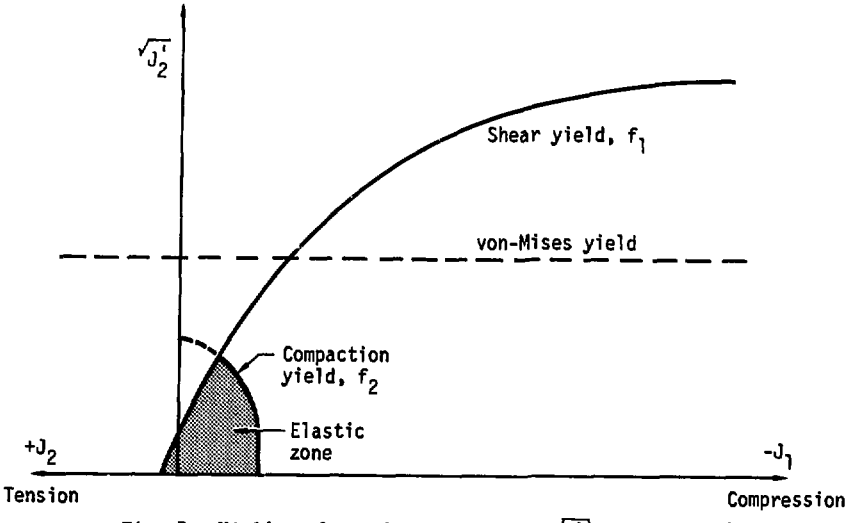

Fig. 7. Yield surfaces for concrete in $\sqrt{J_2'} - J_1$ space.[21]

A,B,C, parameters determined from experimental data.

The $\sqrt{J_2'} - J_1$ axes may also be visualized as shear and pressure. The solid lines representing shear and compaction yield for concrete are in contrast to the von Mises yield surface. Note the continuation of shear-yield surface into tension region.

Results

Three sets of numerical simulations were conducted, the first of which compared the simulated-impact interaction of the missile and target models with experimental-test results. The second assessed the progression of damage for two target thicknesses due to increasing missile velocities. The third set made preliminary examination of the impact interaction of a deformable missile and reinforced-concrete target wall.

COMPARISON WITH EXPERIMENTAL RESULTS

The objective of the first set of simulations was to determine if correlation between experimental and numerically simulated results could be made. Two of Calspan's full-scale tests, Test No. 4F and Test No. 3F, were chosen

for comparison. Both tests involved nondeformable impacting missiles and 12-in., reinforced-concrete target walls.

For the numerical simulations, the key to assessing the damage profile of the modeled concrete target is identifying the back-face, tensile-yield region. Once the time when a specific region first yielded in tension was determined, the surrounding nodal points were then used to determine the potential scabbing velocity of the yield region.

The data used in defining the soil and crushable foam model were based on test results for nonreinforced concrete. As no data were available for steel reinforcement, some assumptions and modifications to parameters were made. The steel reinforcement was essentially smeared in the corresponding concrete zone and was represented by increasing the tensile-yield value.

To assess the effects of the modifications, three preliminary concrete models were evaluated. The first model described the target as a nonreinforced barrier while the second used two modified zones of concrete, representing the front- and back-mat reinforcements. The third model used only one modified layer representing only the back reinforcement, and based on several trials, was chosen as the most appropriate for this study.

NUMERICAL SIMULATION OF CALSPAN TEST NO. 4F

Calspan Test No. 4F is a steel-slug missile impacting a 12-in. reinforced-concrete target at 122 fps. A schematic of the damage is shown in Fig. 8 and a summary of the field test results is given in Table 1. An enlargement of the finite element mesh at the point of impact is noted in Fig. 9.

The back-face elements' mean-stress time histories are shown in Fig. 10. The velocity-time histories of the corresponding back-face nodes are illustrated in Fig. 11.

The diameter of the target wall was selected so that the impacting time would be short, relative to the fundamental period of the target structure. To define the shear-yield surface, the tension-yield limit was set to 255 psi, with the rest of the surface defined by PI's concrete model.[5] The tension-yield limit of the reinforced layer representing the steel reinforcement of the backface was set to 500 psi.

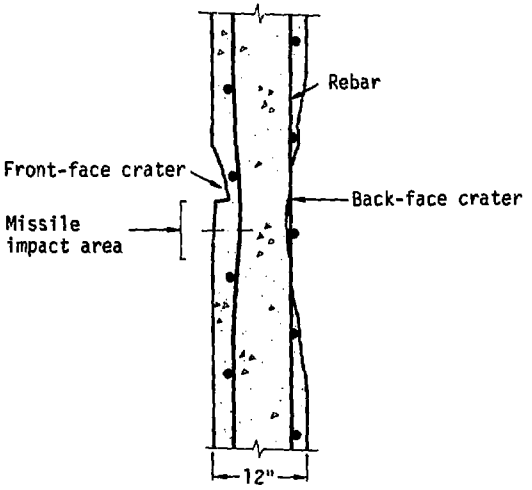

Fig. 8. Damage profile of Calspan Test No. 4F.

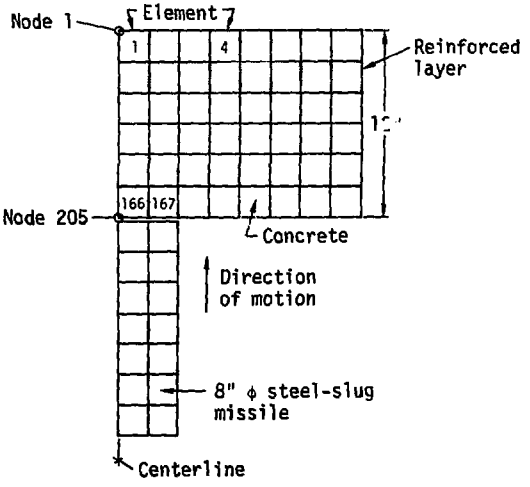

Fig. 9. Finite element mesh at the point of impact.

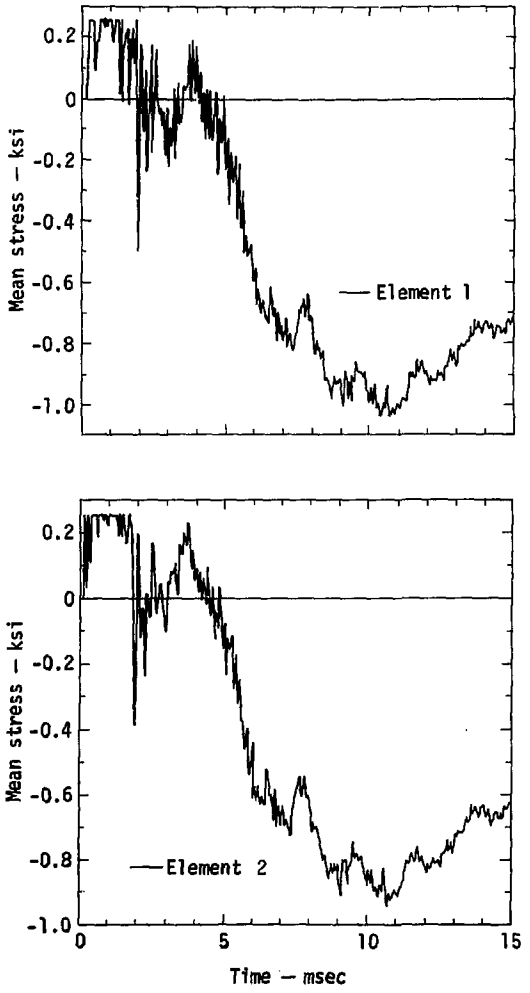

Fig. 10. Test 4F: mean-stress time histories (back-face elements).

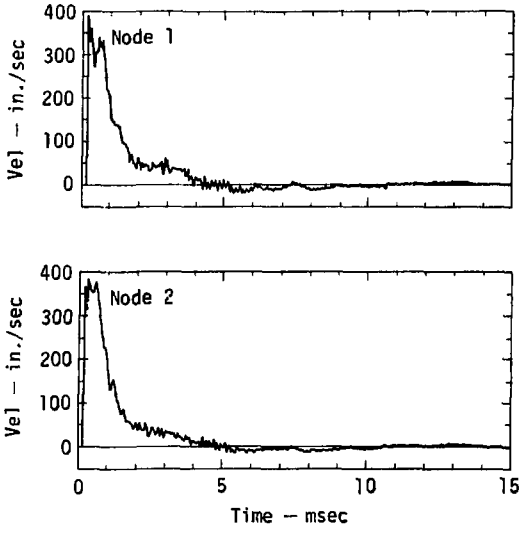

Fig. 11. Test 4F: velocity time histories (back-face nodes).

Table 1. Summary of Calspan Test No. 4F

Missile:	**Panel:**
Type Slug	Thickness, in. 12
Weight, lb 214	Reinf., EWEF(%) 0.4
Length, in. 14	Concrete strength, psi 5770
Velocity (fps) 122	
Results:	
Maximum scab velocity, fps 25	
Penetration depth, in. 0.12 - 0.75	
Front crater diameter, in. 1	
Back crater diameter, in. 45	
Rebound velocity, fps 4	

Within the first 200 μsec after impact, the stress-state of the back-face elements are their limiting tensile-yield value. The stress-state of the back-face elements remain at the upper tensile value for several milliseconds before the succeeding compression waves become dominant. Assuming that the duration of the tensile stress-state is sufficient to cause the back-face elements to scab, we predicted the maximum scabbing velocity to be approximately 32 fps (390 in./sec). This compares with the maximum measured scabbing velocity of 25 fps. The 30% discrepancy between predicted and measured results is reasonable, considering that the maximum scabbing velocity is greatly dependent upon the mass of the scab material and the time when the scab mass breaks away from the target structure. Figure 12 shows the concrete material in the impact area to be in compression throughout the duration of impact, with a peak dynamic compressional stress of 25 ksi.

Element 169 is the element along the perimeter of the impact area. As described by the damage-profile schematic, certain areas along the perimeter of the impact area fail during impact. The perimeter element 169 reaches the tensile-yield limit for a period of a few hundred microseconds before going into a compression stress-state (Fig. 13). Assuming that the duration of a few hundred microseconds is sufficient to cause tensile failure of the concrete material, the concrete model used was adequate in describing the key failure areas of Test No. 4F.

NUMERICAL SIMULATION OF CALSPAN TEST NO. 3F

Calspan Test No. 3F is a steel-slug missile impacting a 12-in., reinforced-concrete target at 214 fps. Summary of the field test results are given in Table 2. The same element mesh used in the simulation of Test 4F was used to simulate Test 3F.

The back-face elements' mean-stress, time histories are depicted in Fig. 14; the velocity-time histories of the back-face nodes are shown in Fig. 15.

The tension-yield limit for this concrete model was set to 250 psi. PI's concrete model was used to define the rest of the shear-yield surface. The tension-yield limit of the reinforced layer was set to 500 psi.

A much wider, back-face damage region was seen in the simulation of Test 3F. This larger damage region was expected since the kinetic energy of the missile was increased and a lower tension-yield limit was used. The

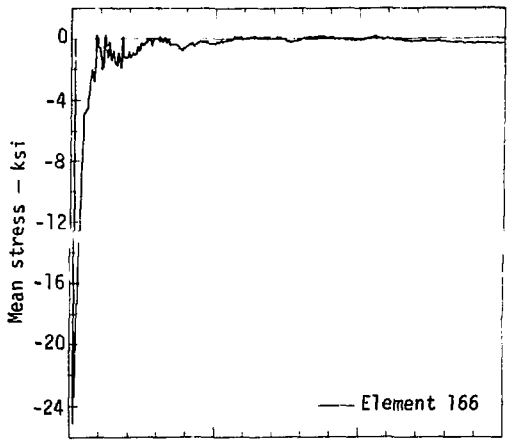

Fig. 12. Test 4F: mean-stress time histories (center of impact).

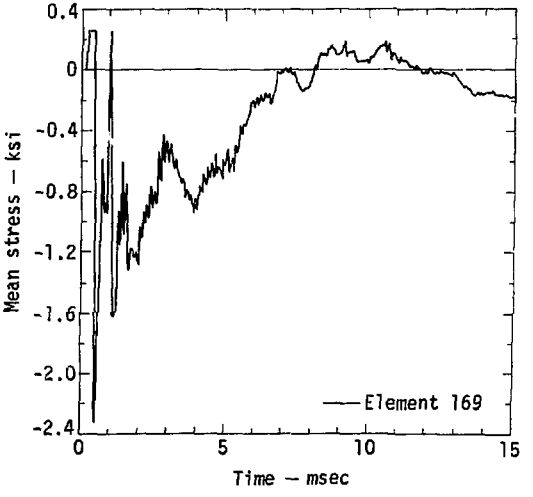

Fig. 13. Test 4F: mean-stress time histories (perimeter impact area).

Table 2. Summary of Calspan Test No. 3F

Missile		Panel:	
Type	Slug	Thickness, in.	12
Weight	214	Reinf., EWEF(%)	0.4
Length, in.	14	Concrete strength, psi	4550
Velocity, fps	214		

Results:	
Maximum scab velocity, fps	105
Front crater diameter, in.	16
Back crater diameter, in.	48
Rebound velocity, fps	10

maximum scabbing velocity was calculated to be 83 fps (1000 in./sec), and was extracted from the velocity-time history of node 2. The maximum measured scabbing velocity was 105 fps.

Figure 16 illustrates the concrete material in the impact area reaching a maximum, dynamic compressional stress of 438 ksi. Figure 17 shows the kinetic, potential and total energy of the system. A perceptible energy loss is apparent. The deform shapes at select times are depicted in Fig. 18. In Table 3, the CPU and I/O cost to simulate this problem are tabulated.

COMPARISON WITH EMPIRICAL FORMULAS

To extend the experiences gained by the numerical simulation of Calspan's experimental tests and to incorporate the findings of SRI's studies[21,9] on the dynamic behavior of concrete, another series of numerical simulations were formulated. The results of these simulations were compared with empirical formulas.

The dimensions and properties for the impacting missile were the same as the steel-slug missile used in the first series of simulations. The selected ultimate strength of the concrete was 5770 psi. The tension-yield limit, chosen as a function of the concrete ultimate strength, was set to 350 psi. Data from SRI's studies on concrete behavior were used to define the remaining shear-yield surface. The tension-yield limit for the reinforced layer was set to 525 psi.

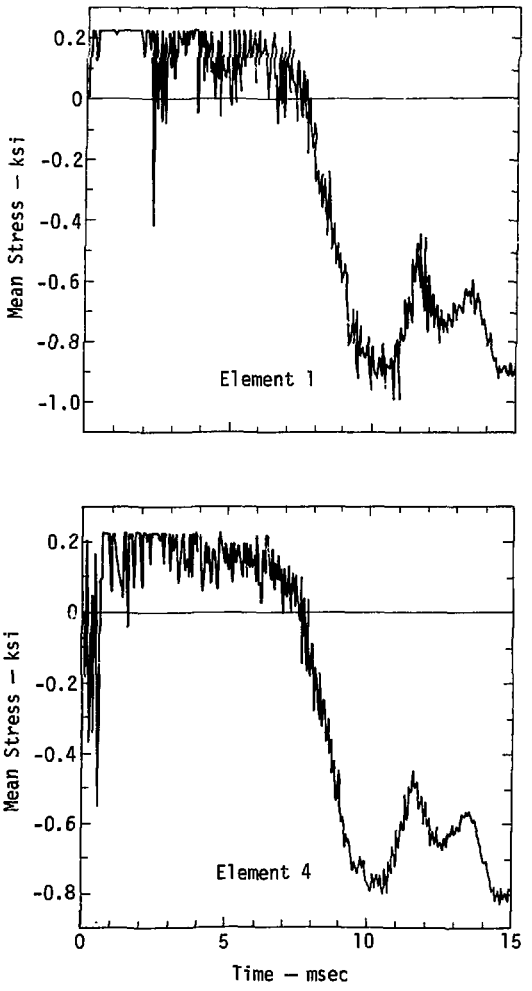

Fig. 14. Test 3F: mean-stress time histories (back-face nodes).

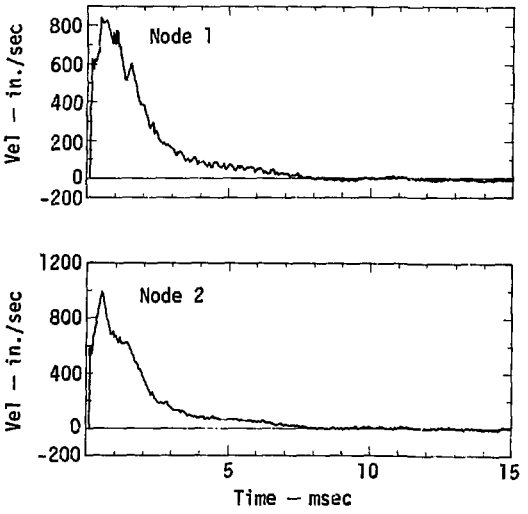

Fig. 15. Test 3F: velocity time histories (back-face nodes).

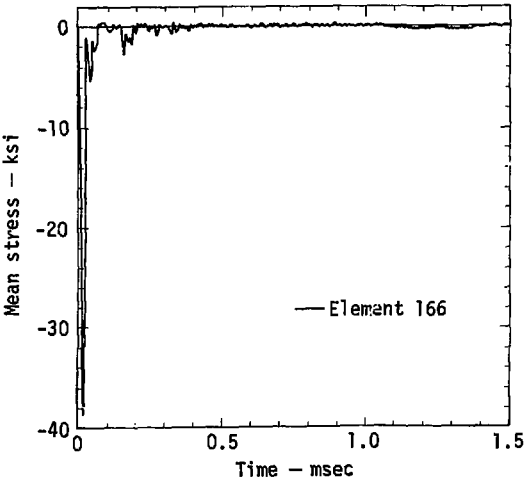

Fig. 16. Test 3F: mean-stress time histories (center of impact).

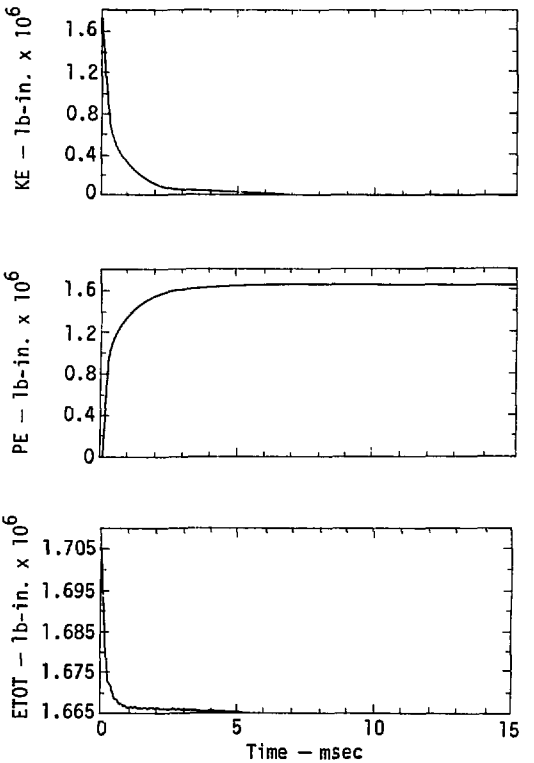

Fig. 17. Test 3F: kinetic, potential and total energy of the system.

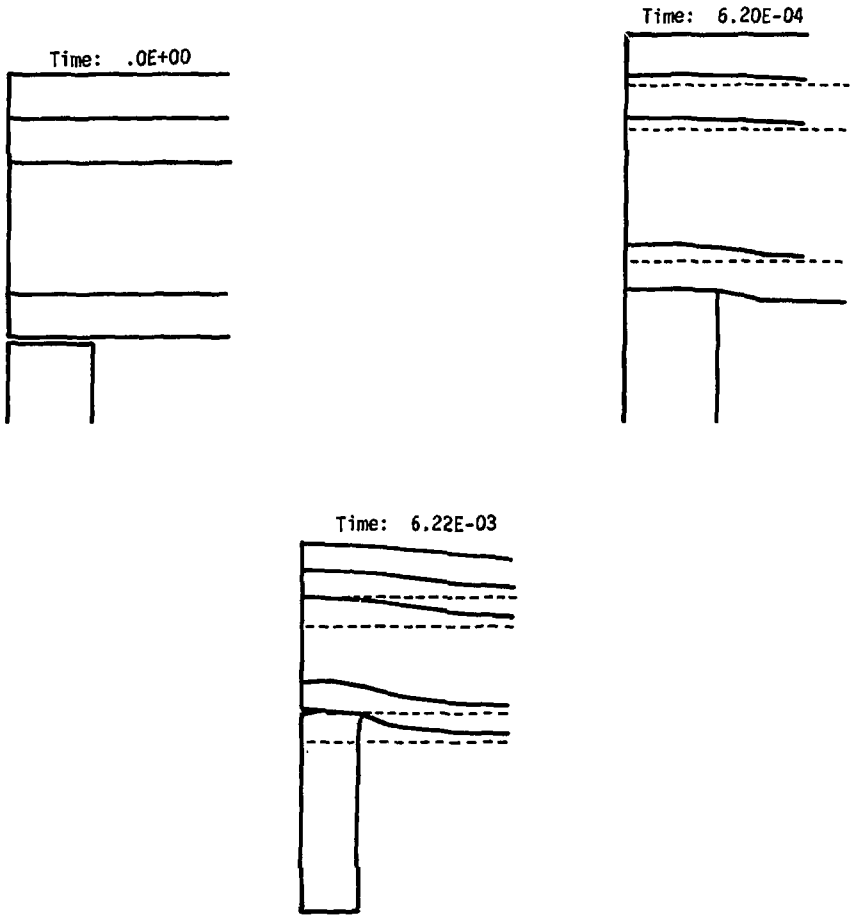

Fig. 18. Test No. 3F: deformed shapes magnified at selected output times.

Table 3. CPU and I/O cost for Test 3F.

Operations	Time, min. CPU	I/O
Initialization	0.005	0.044
Vector updates	3.054	.0
Disk writes	.000	.033
Write output file	.004	.25
Slide and void routines	.018	.0
Total:	3.081	0.103

Four simulations were run, with target walls 12- and 18-in. thick. A summary of the simulations is found in Table 4. The element mesh for test Series A and B are noted in Fig. 19 and Fig. 20.

Results of Test Series A

For both test A1 and test A2, the Modified NDRC and Bechtel formulas indicate that the 12-in.-target wall is adequate to prevent scabbing. The numerical simulations of the two tests show that the back-face elements of the target walls are at or near the scabbing threshold. Fig. 21 illustrates the mean-stress time histories of the back-face elements of test A1 and test A2. For both the tests, a very small region (element 1) has a potential of scabbing No significant duration of tension-yield-limit value is seen in element 4 in both tests.

Figure 22 shows the interface pressures of the frontal impact areas for test A2. Interposed onto the time histories are the Modified NDRC's[10] impact-pressure time histories. As can be seen, the Modified NDRC's maximum predicted interface pressure is a magnitude lower than the maximum value predicted by the finite element method. Modified NDRC also predicts a much longer duration of the interface pressures.

Results of Test Series B

The numerical simulations of the test B1 and test B2 indicate that back-face area has a strong potential of scabbing (Fig. 23). The maximum predicted scabbing velocities for test B1 and B2 are 25 and 50 fps, respectively (Fig. 24).

Table 4. Summary of Test Series A and B.

Test	Missile velocity, fps	Panel thickness, in.	Concrete strength, psi	Predicted scabbing thickness	
				Modified NDRC, in.	Bechtel, in.
A1	67	12	5770	10.64	9.39
A2	75	12	5770	11.16	9.96
B1	200	18	5770	21.23	16.30
B2	275	18	5770	24.39	19.06

For test B1, the Modified NDRC formula agrees that the 18-in. wall will not be adequate to prevent scabbing while the Bechtel formula indicates that the 18-in. is greater than the required scabbing thickness. For test B2, both Modified NDRC and Bechtel formulas indicate that the 18-in.-target wall is not sufficient to prevent scabbing.

DEFORMABLE MISSILE

A preliminary effort was made to simulate numerically the impact interaction of a deformable missile striking a reinforced concrete wall. The selected deformable missile was a 12-in.-diam steel pipe. The pipe weighed 650 lb and was 12 ft long. The missile velocity was set to 91 fps. The element mesh at the point of impact is noted in Fig. 25 while the deformed shapes at selected output times are illustrated in Fig. 26. In Table 5, the CPU and I/O cost to simulate this problem are tabulated.

The mean-stress time histories for the elements along the impact surface of the concrete target are depicted in Figs. 27, 28, and 29. As can be seen by the time histories, the concrete region surrounding the contact area reach their tensile-yield limits immediately after impact of the missile. The concrete elements in direct contact with the impacting missile (Fig. 28) reach a maximum compression stress of 5.5 ksi.

Further simulations of deformable missile impact must be conducted, and comparison of the results with experimental test must be made before assessment of the applicability of the HONDO code can be made for deformable missiles.

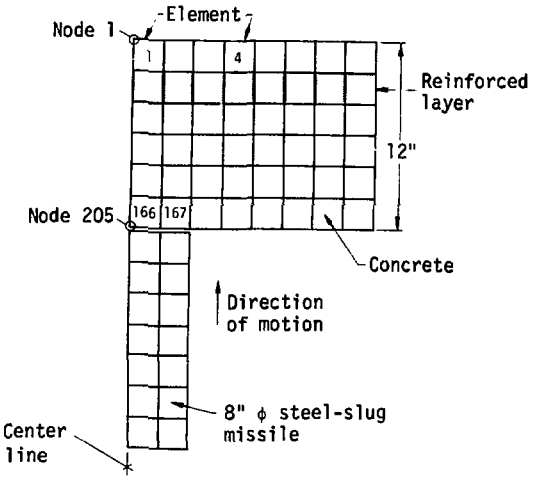

Fig. 19. Series A: element mesh (12-in. wall).

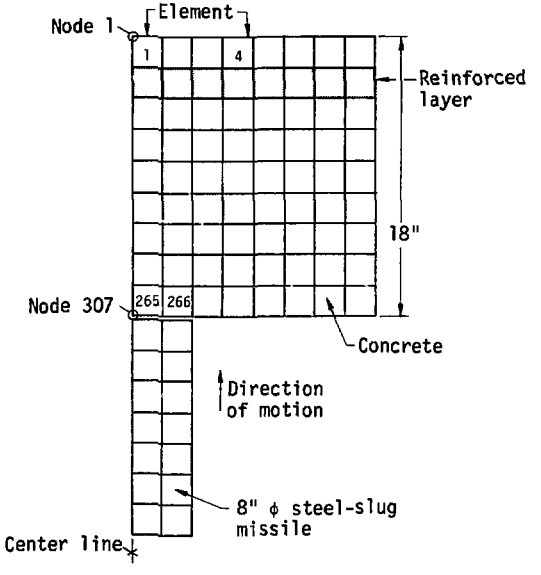

Fig. 20. Series B: element mesh (18-in. wall).

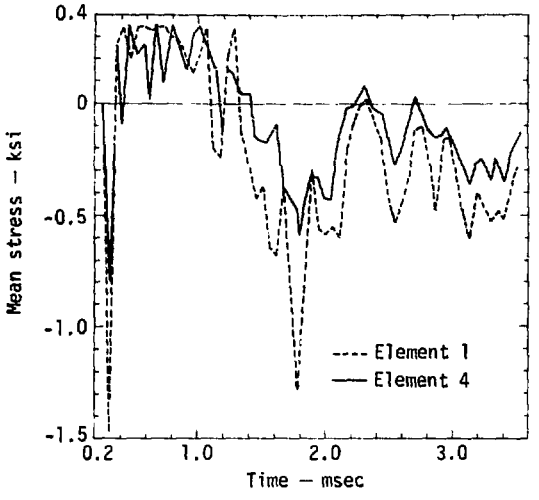

a) Test A1: Missile velocity = 67 fps

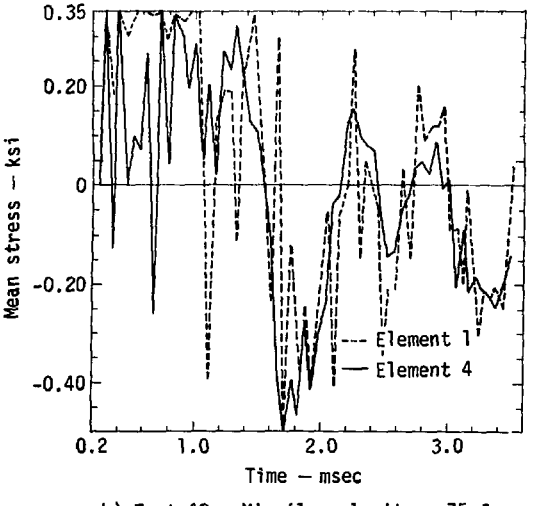

b) Test A2: Missile velocity = 75 fps

Fig. 21. Series A: mean-stress time histories (back-face elements).

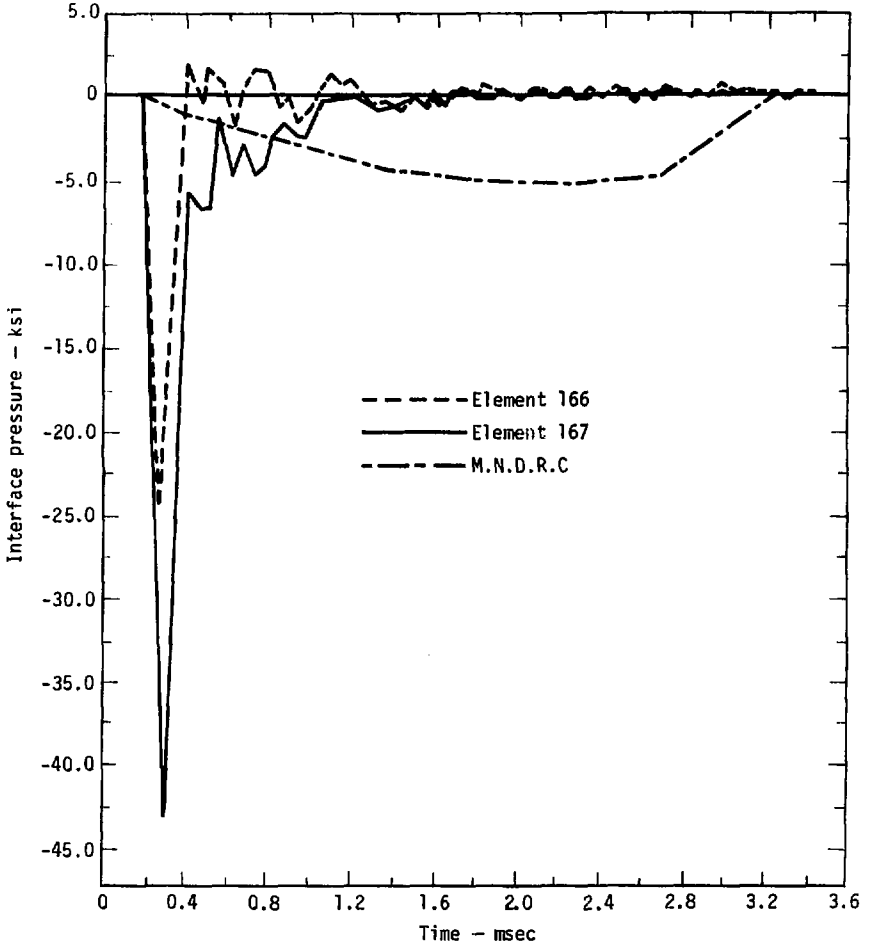

Fig. 22. Test A2: interface-pressure time histories.

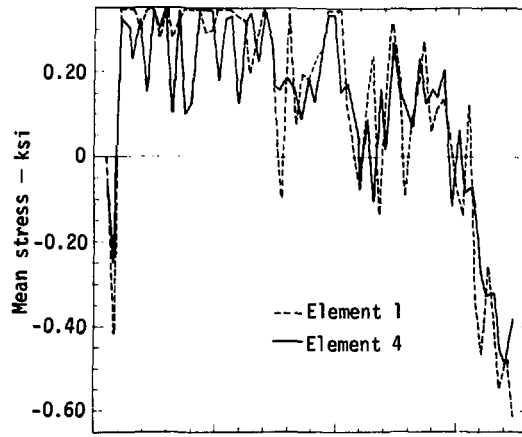

a) Test B1: Missile velocity = 200 fps

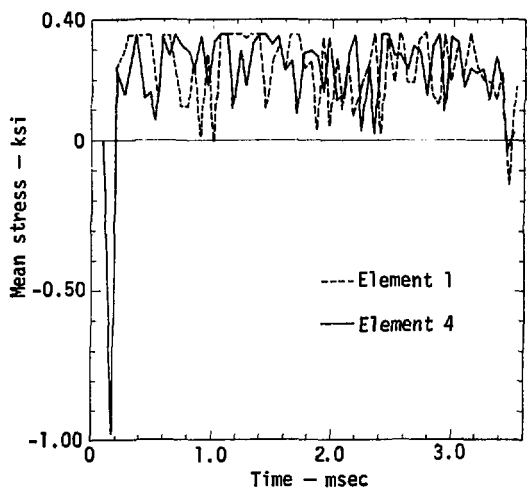

b) Test B2: Missile velocity = 275 fps

Fig. 23. Series B: mean-stress time histories (back-face elements).

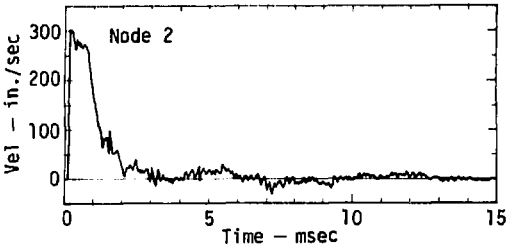

(a) Test B1: Missile velocity = 200 fps

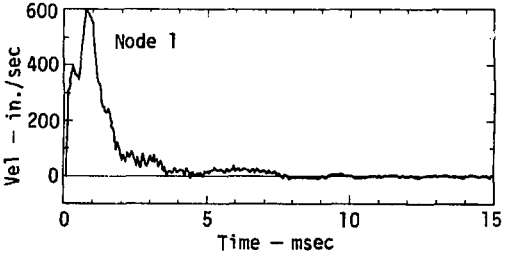

b) Test B2: Missile velocity = 275 fps

Fig. 24. Series B: velocity time histories (back-face nodes).

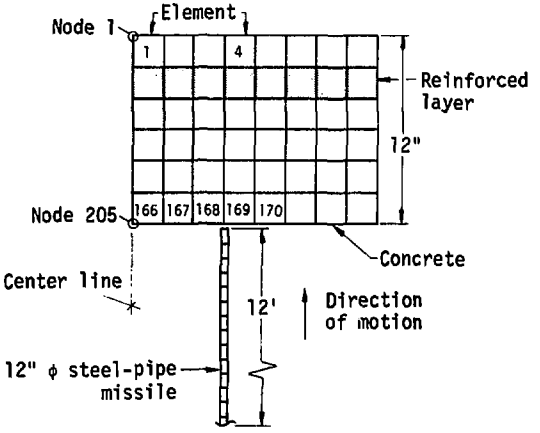

Fig. 25. Finite element mesh for deformable missile.

Conclusions

Constitutive relations do exist to describe the dynamic behavior of the missile and concrete materials. Although the finite element method needs to be further extended to model deformable missiles, it can probably be developed easily into a practical analytical tool in identifying the strength and weakness of present design and analytical methods for tornado-missile impact.

In comparing the full-scale test results with empirical formulas, the Modified NDRC formula and the Bechtel formula were found to be the only equations valid for tornado-type missile. In predicting the scabbing threshold, the finite element method compared closer with the Modified NDRC formula than the Bechtel formula. The recommended 25% increase of Bechtel's formula in predicted scabbing threshold thickness would bring the Bechtel formula in line with the predictions of the Modified NDRC formula and the finite element method.

The interface-pressure time history of the frontal impact area as described by the Modified NDRC method[10] is not supported by the finite element method. The maximum interface pressure predicted by the finite element method

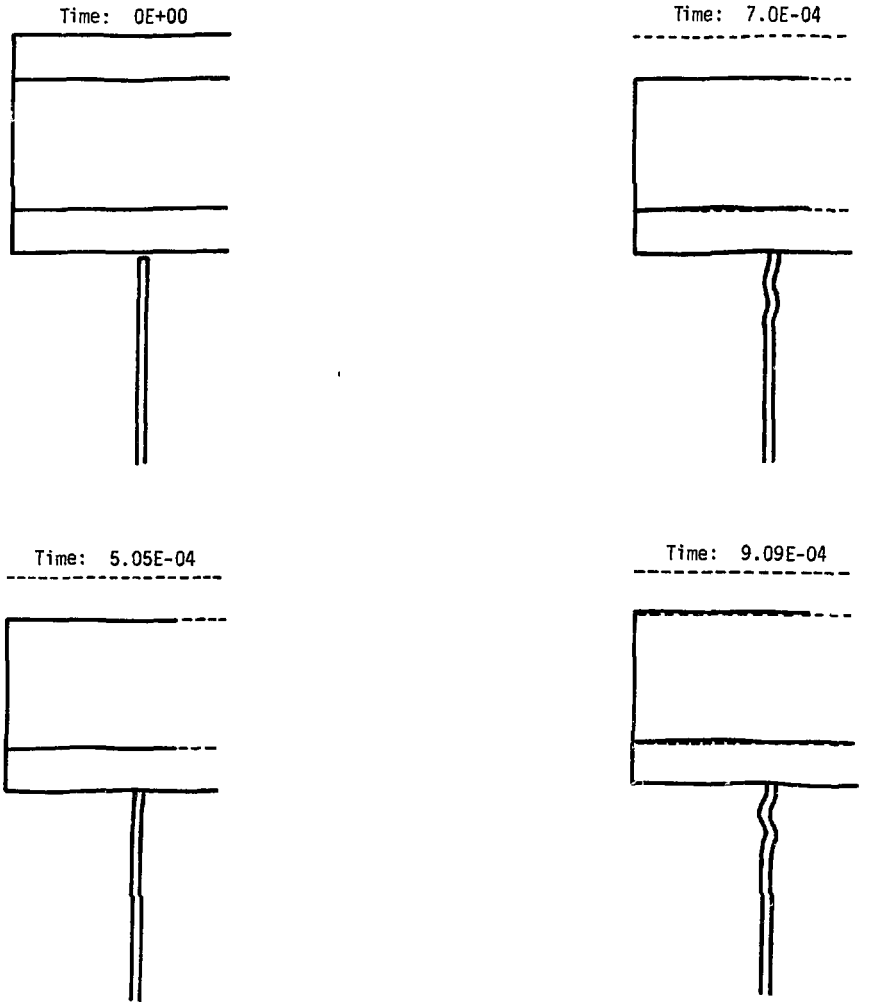

Fig. 26. Deformed shapes at selected output times.

Table 5. CPU and I/O cost for deformable missile simulation.

Operations	Time, min. CPU	I/O
Initialization	0.012	0.689
Vector updates	3.274	.0
Disk writes	.000	.148
Write output file	.002	.016
Slide and void routines	.006	.0
Total:	3.294	0.853

is a magnitude greater than the Modified NDRC's prediction. The interface-pressure duration as predicted by the finite element method is also much shorter.

Further development of the uses of the finite element method toward the problem of tornado-borne missile impacting on reinforced concrete walls should be pursued.

Future Work

Further development is needed before the finite element method will become an acceptable procedure for evaluating the dynamic local response of tornado missile impact. Future work would include:

- Continued correlation of analytical predictions and experimental observations to establish a set of "supporting" calculations.
- Further refinement of the concrete constitutive model to adequately capture concrete's dynamic behavior.
- Failure criteria for shear and compressions before assessing damage in the frontal area.
- Extending further the finite element model to deformable missiles.

Acknowledgment

The authors wish to acknowledge the contributions made by Dr. John Hallquist of the Applied Mechanics Group (Nuclear Explosives Engineering Division), Mechanical Engineering Department. His comments and suggestions have been most helpful.

We also wish to thank A. Stephenson of Sandia Laboratories for giving us a personal tour of his experimental facilities and for providing us with his test results.

Particularly, we wish to thank Dr. J. Costello, U.S. Nuclear Regulatory Commission, Office of Standards Development, for his guidance and support throughout this study.

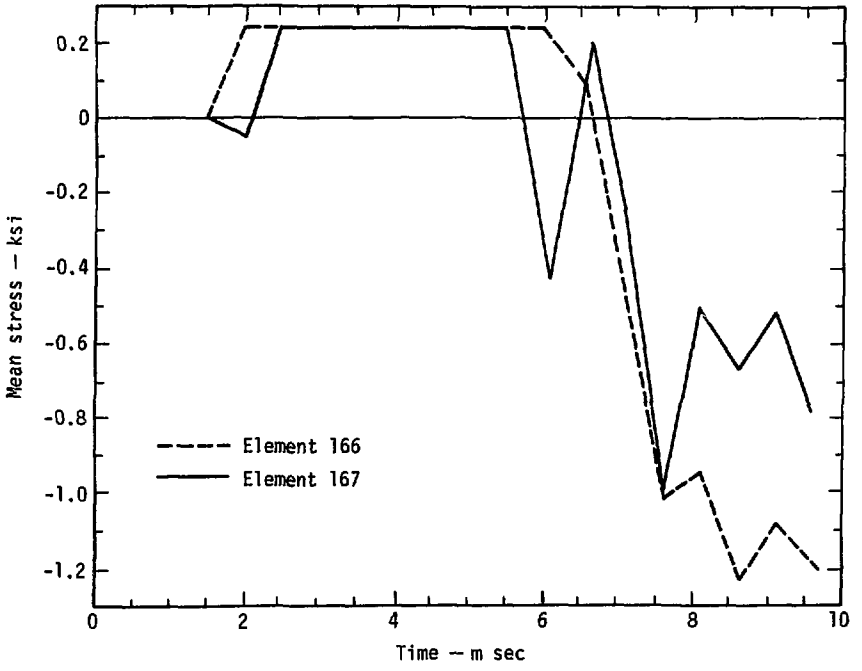

Fig. 27. A 12-in.-diam. pipe: mean-stress time histories (elements 166 and 167).

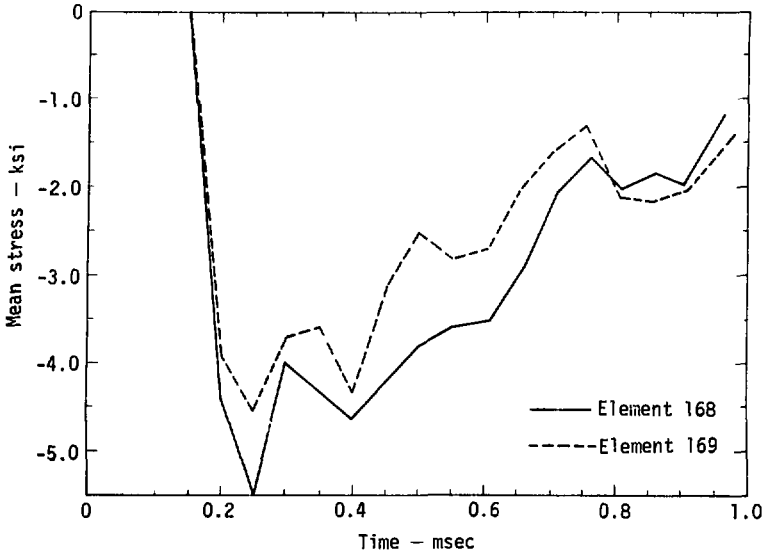

Fig. 28. A 12-in.-diam. pipe: mean-stress time histories (elements 168 and 169).

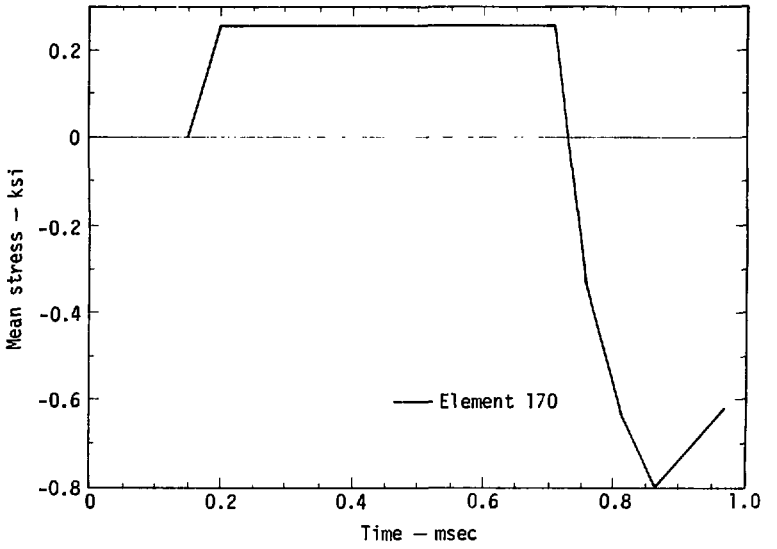

Fig. 29. A 12-in.-diam. pipe: mean-stress time histories (element 170).

References

1. Broman, R., Subramanian, C. V., and Vinson, T. J., "Design of Containment for Impulse and Impact Loads," *Proceedings of the Specialty Conference on Code Requirements for Nuclear Containments*, Chicago, Illinois, Dec. 9-10 (1974).
2. *Design Basis Tornado for Nuclear Power Plants, Regulatory Guide 1.76*, U.S. Atomic Energy Commission (April 1974).
3. *Standard Review Plan: Missiles Generated by Natural Phenomenon Section 3.5.1.4*, U.S. Nuclear Regulatory Commission, Office of Nuclear Reactor Regulation (June 1975).
4. Bernard, Robert and Hanagud, S.V., *Development of a Projectile Penetration Theory, Report 1, Penetration Theory for Shallow to Moderate Depth*, U.S. Army Engineer, Waterway Experiment Station (June 1975).
5. *Dynamics of a Burnt Projectile Impacting Concrete at 1400 Feet Per Second*, Physics International Co., San Leandro, Calif. (April 1975).
6. Tillerson, J. R., *Numerical Modeling of Containment Wall Impact by Tornado Generated Missiles — Preliminary Results.* Sandia Laboratories, Albuquerque, New Mexico (March 1975).
7. *Structures to Resist the Effects of Accidental Explosions*, Department of the Army, the Navy, and the Air Force, Tech Manual TM 5-1300 (June 1969).
8. Rotz, J. V., "Results of Missile Impact Tests on Reinforced Concrete," *Second Specialty Conference on Structural Design of Nuclear Plant Facilities*, New Orleans, Louisiana, December 8-10 (1975).
9. Gupta, Y. M. and Seaman, L., *Development of Dynamic Constitutive Relation for Reinforced Concrete*, Stanford Research Institute, Menlo Park, Calif. (Nov. 1975).
10. Kennedy, R. P., *A Review of Procedures for the Analysis and Design of Concrete Structures to Resist Missile Impact Effects*, Holmes and Narver, Inc., Anaheim, Calif. (September 1975).
11. Vassallo, F. A., *Missile Impact Testing of Reinforced Concrete Panel Calspan Corporation*, Buffalo, New York (January 1975).
12. Stephenson, Alan, *Tornado Vulnerability Nuclear Production Facilities*, Sandia Laboratories, Albuquerque, New Mexico (April 1975).
13. Stephenson, Alan, *Full Scale Tornado Missile Impact Tests, EPRI NP-14B*, Sandia Laboratories, Tonopah, Nevada (April 1976).

14. Stephenson, Alan, *Full Scale Tornado Missile Impact Tests*, EPRI NP-330, Sandia Laboratories, Tonopah, Nevada (August 1976).

15. Key, S. W., *HONDO – A Finite Element Computer Program for Large Deformation Dynamic Response of Axisymmetric Solids*, Sandia Laboratories, Albuquerque, New Mexico (April 1974).

16. Hallquist, J., *A Procedure for the Solution of Finite-Deformation Contact – Impact Problems by Finite Element Method*, Lawrence Livermore Laboratory, Livermore, Calif. (April 1976).

17. Argyis, J. H., Faust, G., and William, K. J., "Unified Stress-Strain Law for Triaxial Concrete Failure," *3rd Post Conference on Computational Aspects of the Finite Element Method*, Imperical College, London, England, September 8-9 (1975).

18. Attalla, J., and Nowotny, B., "Missile Impact on a Reinforced Concrete Structure," *Nuclear Engineering and Design*, 37 (1976).

19. Birkmer, D. and Lindeman, R., "Dynamic Tensile Strength of Concrete Materials," *Journal of the American Concrete Institute*, 68 (Jan. 1971).

20. Read, H. E., *The Dynamic Behavior of Concrete*, Systems Science and Software, La Jolla, Calif. (August 1971).

21. Gupta, Y. M. and Seaman, L., *A Generalized Plasticity Model for Predicting Failure of Concrete*, Stanford Research Institute, Menlo Park, Calif. (Feb. 1976).

LRS/gw